SnT 2019
CTBT: SCIENCE AND TECHNOLOGY CONFERENCE

USC University of Southern California

Representation of Complex Seismic Sources by Orthogonal Moment Tensor Fields

Alan Juarez & Thomas H. Jordan
Department of Earth Sciences, University of Southern California, Los Angeles, CA.

T2.1-P23

Introduction

Complexity of seismic sources can be represented by space-time variations of stress gluts. We present a new representation theorem of seismic sources that exactly and uniquely decomposes any stress-glut density into a set of up to six orthogonal tensor fields of increasing degree (Jordan & Juarez, GJI-2019):

- This representation generalizes the point-source approximation to a sum of multipoles. The centroid moment tensor (CMT) as its 0th-degree term.
- The total scalar moment M_T is the integral of the scalar moment density.
- We estimate moments for each degree. If the source is complex, M_T is larger than M_0, the Aki moment.

We decompose seismic source models of earthquakes and explosions to illustrate how the higher-degree terms characterize the source complexities. Synthetic seismograms illustrate the radiation patterns of the higher-degree fields.

Our results indicate that the radiation from the higher-degree fields is large enough that it may be possible to estimate low-order multipoles directly from seismic data.

Representation of Mechanism Complexity

1. Sum of CMT point sources:

$$\dot{\mathbf{\Gamma}}(\mathbf{x}) = \sum_{n=1}^{N} \sqrt{2}\, M_n\, \widehat{\mathbf{M}}_n\, \delta(\mathbf{x}-\mathbf{x}_n)$$

2. Sum of orthogonal moment-tensor fields:

$$\dot{\mathbf{\Gamma}}(\mathbf{x}) = \sum_{\alpha=0}^{D-1} \widehat{\mathbf{M}}_\alpha\, g_\alpha(\mathbf{x})$$

where $\widehat{\mathbf{M}}_\alpha : \widehat{\mathbf{M}}_\beta = \delta_{\alpha\beta}$,
D is the dimensionality, and
$g_\alpha(\mathbf{x}) = \widehat{\mathbf{M}}_\alpha : \dot{\mathbf{\Gamma}}(\mathbf{x}) = \sqrt{2}\, m(\mathbf{x}) \cos\theta_\alpha(\mathbf{x})$

The total moment:

$$M_T = \int_{\mathcal{V}} m(\mathbf{x})\, d\mathbf{x} = \frac{1}{\sqrt{2}} \int_{\mathcal{V}} \|\dot{\mathbf{\Gamma}}(\mathbf{x})\|\, d\mathbf{x}$$

Aki moment:

$$M_0 = \int_{\mathcal{V}} m(\mathbf{x}) \cos\theta_0(\mathbf{x})\, d\mathbf{x}$$

Fractional moments:

$$\acute{M}_\alpha = \int_{\mathcal{V}} m(\mathbf{x}) \cos^2\theta_\alpha(\mathbf{x})\, d\mathbf{x}$$

Planar Fault Examples (D=2)

Model: double-couple distribution on a planar fault with one rotational degree of freedom

$$\boldsymbol{\mu}^{(0)}(\dot{\mathbf{\Gamma}}) = \sqrt{2}\, M_0\, \widehat{\mathbf{M}}_0 = M_0(\hat{\mathbf{n}}_0\, \hat{\mathbf{s}}_0 + \hat{\mathbf{s}}_0\, \hat{\mathbf{n}}_0)$$

Rake variations:

$\hat{\mathbf{s}}(\mathbf{x}) = \hat{\mathbf{s}}_0 \cos\theta(\mathbf{x})$
$\widehat{\mathbf{M}}_1 = \frac{1}{\sqrt{2}} (\hat{\mathbf{n}}_0\, \hat{\mathbf{b}}_0 + \hat{\mathbf{b}}_0\, \hat{\mathbf{n}}_0)$
$\dot{\mathbf{\Gamma}}(\mathbf{x}) = \sqrt{2}\, m(\mathbf{x})\, [\widehat{\mathbf{M}}_0 \cos\theta(\mathbf{x}) + \widehat{\mathbf{M}}_1 \sin\theta(\mathbf{x})]$

Strike variations:

$\hat{\mathbf{s}}(\mathbf{x}) = \hat{\mathbf{s}}_0 \cos\varphi(\mathbf{x}) - \hat{\mathbf{n}}_0 \sin\varphi(\mathbf{x})$,
$\hat{\mathbf{n}}(\mathbf{x}) = \hat{\mathbf{s}}_0 \cos\varphi(\mathbf{x}) + \hat{\mathbf{n}}_0 \sin\varphi(\mathbf{x})$
$\widehat{\mathbf{M}}_1 = \frac{1}{\sqrt{2}} (\hat{\mathbf{s}}_0\hat{\mathbf{s}}_0 - \hat{\mathbf{n}}_0\, \hat{\mathbf{n}}_0) = \frac{1}{\sqrt{2}} (\hat{\mathbf{t}}_0\hat{\mathbf{p}}_0 + \hat{\mathbf{p}}_0\, \hat{\mathbf{t}}_0)$
$\dot{\mathbf{\Gamma}}(\mathbf{x}) = \sqrt{2}\, m(\mathbf{x})\, [\widehat{\mathbf{M}}_0 \cos 2\varphi(\mathbf{x}) + \widehat{\mathbf{M}}_1 \sin 2\varphi(\mathbf{x})]$

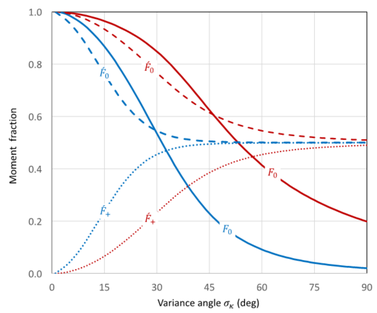

Figure 1. Moment fractions F_0 (solid), $\acute{F}_0$ (dashed), and $\acute{F}_+$ (dotted) as a function of variance angle $\sigma_\kappa = 1/\sqrt{\kappa}$ for the von Mises model with in-plane slip (red curves) and the von Mises model with out-of-plane slip (blue curves).

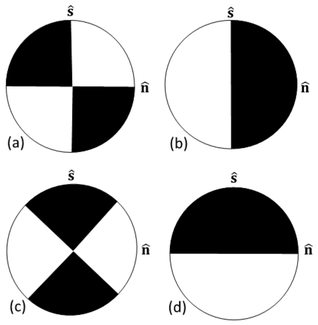

Figure 2. Double-couple source mechanisms for the planar fault models plotted as focal spheres projected onto the $\hat{\mathbf{n}}$-$\hat{\mathbf{s}}$ plane. (a) $\widehat{\mathbf{M}}_0$ (b) $\widehat{\mathbf{M}}_1$ for rake variations. (c) $\widehat{\mathbf{M}}_1$ for strike variations. (d) $\widehat{\mathbf{M}}_1$ for dip variations.

Complex Fault – Graves & Pitarka (2016)

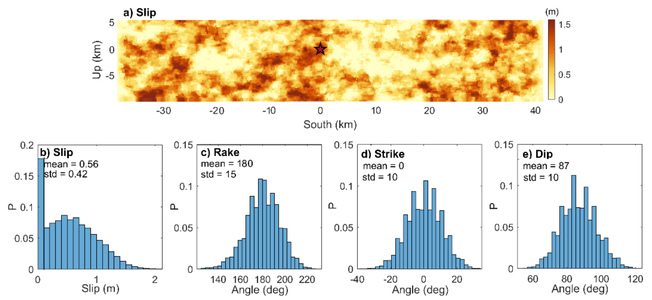

Figure 3. GP-16 kinematic rupture simulator. M_w 6.85, strike-slip, right-lateral earthquake. Rectangular simulation grid of 80 km × 15 km, 0.25 km node spacing and a 0.1 s time sampling. (a) Total slip in meters; red star is the hypocenter. (b)-(e) angular distribution of slip, rake, strike, and dip. Their mean and standard deviations in degrees.

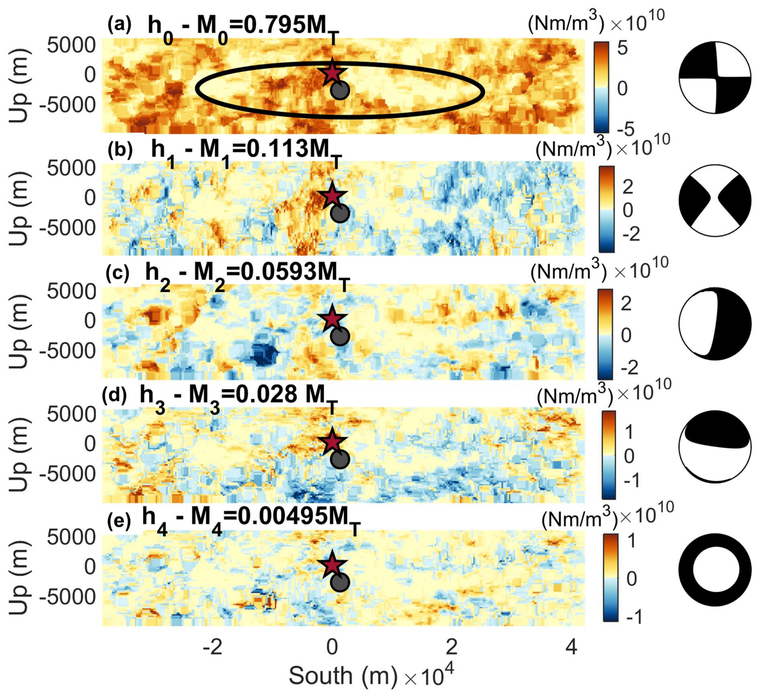

Figure 4. PCA representation of the stress-glut density from Fig. 3. The panel plots (a)-(e) show the time integral of g_α as a function of position on the fault and their source mechanism $\widehat{\mathbf{M}}_\alpha$, respectively, as a focal sphere in plane view (compressional in black; dilational in white). Red star is the hypocenter. (a) g_0 field: circled dot is the spatial centroid $\mathbf{r}_0$ obtained from $\boldsymbol{\mu}^{(1)}(g_0)$; ellipse axes measure the characteristic source dimensions from $\boldsymbol{\mu}^{(2)}(g_0)$.

Source Complexity and Dimensionality

We define $\widetilde{D}$, the effective dimensionality for $\acute{M}_\alpha > 5\% M_T$

Dimensionality is one criteria for complexity. It's defined by the moment fractions, e.g., from the PCA representation of GP-16 $\widetilde{D} = 3$:

Table. PCA $\acute{M}_\alpha$ for the GP-16 model $L = 47.8$ km, $J^{(0)} = 2.19 \times 10^{19}$ Nm

α	$\acute{F}_\alpha$	p = 0	1	2	3	4
0	*0.795*	1.0000	0.0000	0.2532	0.0695	0.1078
1	*0.113*	0.0281	0.0475	0.0212	0.0123	0.0094
2	*0.059*	0.0053	0.0053	0.0057	0.0046	0.0022
3	*0.028*	0.0112	0.0061	0.0047	0.0050	0.0076
4	*0.005*	0.0028	0.0012	0.0009	0.0004	0.0005

$\mu_\alpha^{(p)}/(J^{(0)}L^p)$

Wavefields

The displacement field is

$$\mathbf{u}(\mathbf{x}) = \int_{\mathcal{V}} \mathbf{H}(\mathbf{x};\mathbf{x}') : \dot{\mathbf{\Gamma}}(\mathbf{x}')\, d\mathbf{x}'$$

where $H_{ijn} = \frac{1}{2}(\partial_i' G_{jn} + \partial_j' G_{in})$ is the Strain Green Tensor.

Expanding in a Tylor series about $\mathbf{x}^*$:

$$\mathbf{H}(\mathbf{x};\mathbf{x}') = \sum_{p\geq 0} \frac{1}{p!} (\mathbf{x}'-\mathbf{x}^*)^p\, \boldsymbol{\nabla}_{\mathbf{x}^*}^p \mathbf{H}(\mathbf{x};\mathbf{x}^*)$$

From the Stress-Glut Representation

$$\dot{\mathbf{\Gamma}}(\mathbf{x}) = \sum_{\alpha=0}^{D-1} \widehat{\mathbf{M}}_\alpha\, g_\alpha(\mathbf{x})$$

And the expression for $\mathbf{H}(\mathbf{x};\mathbf{x}')$, we find:

$$\mathbf{u}(\mathbf{x}) = \sum_{p\geq 0} \sum_{\alpha \leq p} \frac{1}{p!} \boldsymbol{\nabla}_{\mathbf{x}}^p \mathbf{H}(\mathbf{x};\mathbf{x}^*) : \widehat{\mathbf{M}}_\alpha \boldsymbol{\mu}^{(p)}(g_\alpha)$$

Table 2. Structure of Moment Array

$\alpha \backslash p$	0	1	2	3
$\widehat{\mathbf{M}}_0$	$J^{(0)}$	$\boldsymbol{\mu}_0^{(1)}$	$\boldsymbol{\mu}_0^{(2)}$	$\boldsymbol{\mu}_0^{(3)}$
$\widehat{\mathbf{M}}_1$	**0**	$\mathbf{J}^{(1)}$	$\boldsymbol{\mu}_1^{(2)}$	$\boldsymbol{\mu}_1^{(3)}$
$\widehat{\mathbf{M}}_2$	**0**	$\boldsymbol{\varepsilon}_2^{(1)}$	$\mathbf{J}^{(2)}$	$\boldsymbol{\mu}_2^{(3)}$
$\widehat{\mathbf{M}}_3$	**0**	$\boldsymbol{\varepsilon}_3^{(1)}$	$\boldsymbol{\varepsilon}_3^{(2)}$	$\mathbf{J}^{(3)}$

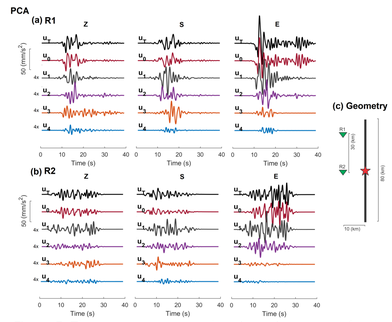

Figure 5. Three-component acceleration seismograms for the source fields of Fig. 4. Seismograms are computed using whole-space Green's functions. (a) Seismograms at R1 in vertical (Z), south (S), and east (E) components. (b) Seismograms at R2. (c) Source and receiver geometry.

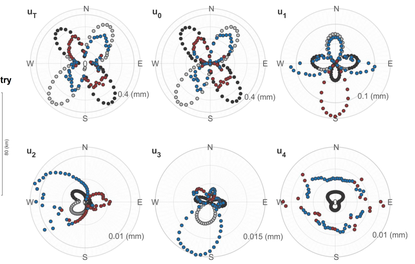

Figure 6. P-waves amplitudes as a function of the azimuth for the model in Fig. 4. Amplitudes are measured in a circular array of 72 receivers at 300 km from the source epicenter. A low-frequency pattern from seismograms band-passed at 0.02-0.1 Hz (black points compressional, gray points dilatational), and a high-frequency pattern from seismograms band-passed at 0.1-1.0 Hz (red points compressional, blue points dilatational).

Explosion Model – Johnson & Sammis (2001)

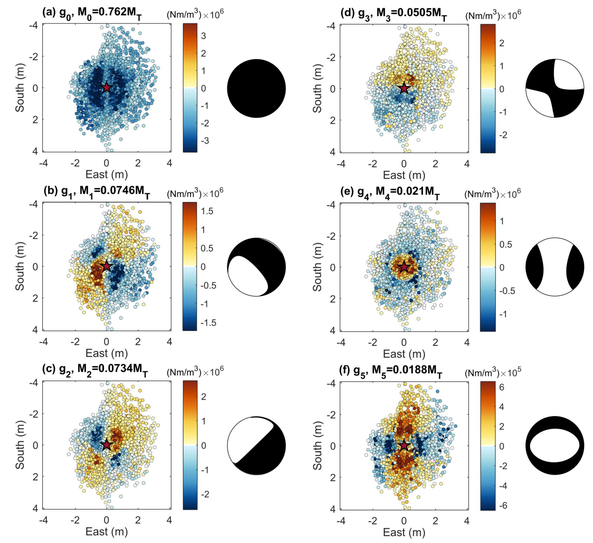

Figure 7. Representation of the stress-glut density from a explosion model (Rogers-Martínez, 2019) using PCA. The panel plots (a)-(f) show the time integral of g_α and their source mechanism $\widehat{\mathbf{M}}_\alpha$ as a focal sphere in plane view (compressional in black; dilational in white). Red star is the explosion centroid.

$\widetilde{D} = 4$ for the explosion model.

Disclaimer: The views expressed on this poster are those of the author and do not necessarily reflect the view of the CTBTO